

# ACTIVIA: Calculation of isotope production cross-sections and yields

J. J. Back\*, Y. A. Ramachers

*Department of Physics, University of Warwick, Coventry, CV4 7AL, United Kingdom*

---

## Abstract

We present a C<sup>++</sup> computer package, ACTIVIA, that can calculate target-product cross-sections and the production and decay yields of isotopes from cosmic ray activation using data tables and semi-empirical formulae. We describe the structure and user interface of the computer code as well as provide comparisons between the calculations and experimental results. We also outline suggestions on how the code can be improved and extended for other applications.

*Keywords:* ACTIVIA; Isotope production; Cosmic rays

*PACS:* 13.85.Tp; 25.40.-h; 25.40.Sc

---

## 1. Introduction

There are many observations made in astrophysics, astronomy and particle physics that require knowledge of the cross-sections of nuclear processes at high energies. The physics of cosmic rays is one example. Understanding how they interact with matter allows us to study the composition of the interstellar medium, the Galaxy and the solar system. Estimating the cosmic ray background radiation in spacecraft and isotope production in accelerator facilities are other important applications. For the case of low background experiments, it is necessary to know which isotopes are formed by cosmic ray activation inside target materials before they are shielded underground. Any long-lived isotopes must be accounted for in the signal data analysis, and this requires information about cross-sections and production rates. There are measurements available for use in such studies, but normally only for a restricted energy range which does not cover the total energy spectrum of the input beam. Some important reactions for low background experiments, such

as <sup>60</sup>Co produced from natural tellurium by cosmic ray activation, have essentially no experimental data available. Accordingly, a set of semi-empirical formulae have been developed by Silberberg and Tsao [1,2] to estimate the cross-sections of various nuclear processes, such as spallation and fission, which can be used to calculate the production yields of nuclear isotopes from cosmic ray activation. The parameters in the formulae, assumed to be the same for proton and neutron beams, have been tuned to best fit the available experimental results.

In this paper we describe a new C<sup>++</sup> package, ACTIVIA, that uses a combination of semi-empirical formulae and tables of data based on experimental results to calculate the cross-section, production rates and yields of radioactive isotopes from cosmic ray activation. Section 2 describes the Silberberg-Tsao semi-empirical formulae used for the cross-section calculations while Section 3 explains how cross-sections can be evaluated if tables of data (in ASCII text format) are available. Section 4 provides details on how the radioactive decay yields are calculated, Section 5 explains the basic structure of the code, while Section 6 shows comparisons between the calculations and experimental data. Finally, in Section 7 we describe possible modifications and extensions that could be made to the code if other in-

---

\* Corresponding author.

*Email addresses:* J.J.Back@warwick.ac.uk (J. J. Back), Y.A.Ramachers@warwick.ac.uk (Y. A. Ramachers).

put beam spectra or nuclear physics processes are required.

## 2. Semi-empirical formulae

We use the extensive set of semi-empirical formulae from Silberberg and Tsao [1,2] to calculate cross-sections for isotope production when a proton or neutron beam (e.g. cosmic rays) hits a given target. The general form of the cross-section equation for a product ( $Z, A$ ) from a target ( $Z_t, A_t$ ) is

$$\sigma = \sigma_0 f(A) f(E) e^{-P\Delta A} \times \exp(-R|Z - SA + TA^2 + UA^3|^\nu) \Omega \eta \xi, \quad (1)$$

where  $E$  is the beam energy (in units of MeV),  $\Delta A$  is the difference between the target and product mass numbers ( $A_t - A$ ), while  $f(A)$  and  $f(E)$  are correction factors usually applied for heavy targets ( $A_t > 30$ ) and when  $\Delta A$  is large ( $\gtrsim 10$ ). The normalisation factor  $\sigma_0$  is the cross-section (in millibarns) at the energy  $E_0$  ( $\sim 3$  GeV), above which cross-sections are assumed to be independent of energy. The first exponential term describes the reduction of the cross-section as  $\Delta A$  increases, where  $P$  is a function of target mass  $A_t$  and  $E$ . The second exponential term describes the distribution of cross-sections for several isotopes for a given element of atomic number  $Z$ ; its parameters ( $R, S, T, U$  and  $\nu$ ) are, in general, functions of target and product  $Z$  and  $A$  values as well as energy. The parameter  $R$  represents the width of the cross-section distribution amongst the isotopes, while  $S$  describes the peaks for various mass numbers  $A$ . The parameter  $T$  describes the increase in the number of neutrons as  $A$  increases, while  $U$  is equal to  $3.0 \times 10^{-7}$  and represents a small correction to improve the overall agreement with available experimental data. The power exponent  $\nu$  varies from 1.3 to 2.0 depending on the target and product isotopes. The parameter  $\Omega$  represents a nuclear structure factor,  $\eta$  is a nuclear pairing factor (for even and odd  $Z$  and neutron ( $N$ ) numbers), while  $\xi$  is an enhancement factor for light evaporation products; these parameters are of order unity. We assume that Eq. 1 is applicable to both proton and neutron beams, with identical formulae and parameters.

Figure 1 shows the various regions for different hadronic processes which can be calculated using Eq. 1 and which are implemented in the computer code. See Silberberg and Tsao [1,2] for detailed information about the parameterisations of the various factors in Eq. 1. The code also calculates the cross-sections for tritium production using the formulae from Konobeyev and Korovin [3].

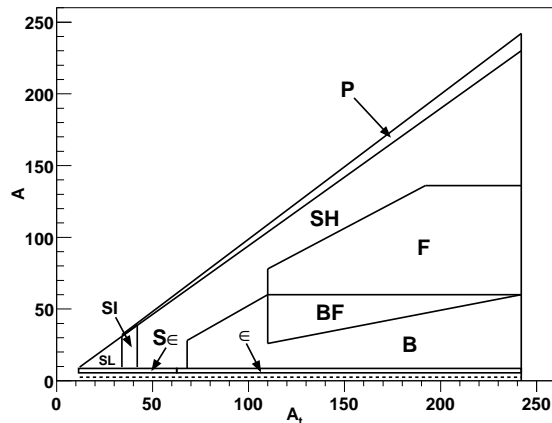


Fig. 1. Domains of applicability of different parameters of Eq. 1 as a function of target mass  $A_t$  and product mass  $A$ , which are implemented in the code. P denotes the reactions that are mainly peripheral; SL, SI and SH denote the spallation of light, intermediate and heavy targets, respectively. The fission region (including contributions from spallation reactions) is denoted by F, the symbol B represents the breakup region in which light nuclei are evaporated, while BF represents the combination of fission and breakup reactions. The evaporation of light nuclei occurs in region  $\epsilon$ , with  $S\epsilon$  combining evaporation and spallation processes. These are the same regions as those in Ref. [1]. Finally, the dotted line represents the tritium production region [3].

## 3. Data tables

There are extensive sets of nuclear data (e.g. the EXFOR database [4]) that can be used to provide cross-sections as a function of energy for target-product isotope pairs. If present, these (ASCII text) tables are used instead of the semi-empirical formulae. A linear interpolation is performed between data points to provide the cross-section (in mb) at a given beam energy (in MeV). It is important that the data be in the correct units, have enough energy bins to be useful and have a contiguous, increasing energy range. Equation 1 is used to calculate the cross-section if any data value is below a selectable lower limit (recommended to be set at 0.001 mb). If two or more separate energy regions are needed, then the data from these must be combined into the same table. For the case of large energy differences in between neighbouring regions, it is sensible to set the cross-sections to zero just above and below the range limits in the table so that the semi-empirical formulae are used instead. Otherwise, the linear interpolation would only give a weighted average of the cross-sections between the data limits of neighbouring energy regions, which may not be reliable enough. The code can use MENDL-2P tables [5] for

intermediate energy (up to 200 MeV) cross-sections.

#### 4. Radioactive decay yields

Consider a target comprised of several isotopes with the same atomic number  $Z_t$  but having different mass numbers  $A_{ti}$  each with a relative abundance fraction  $f_i$  such that  $\sum_i f_i = 1$ . This target is exposed to a beam with an energy spectrum  $d\phi/dE$  ( $\text{cm}^{-2} \text{s}^{-1} \text{MeV}^{-1}$ ), such as cosmic ray neutrons shown in Fig. 2, which is based on the parameterisation from Armstrong [6] and Gehrels [7]. The

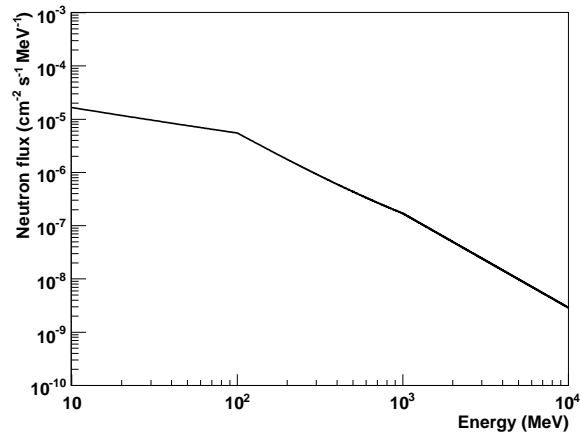


Fig. 2. Energy spectrum for cosmic ray neutrons at sea level based on the parameterisation from Armstrong [6] and Gehrels [7].

production rate ( $\text{kg}^{-1} \text{day}^{-1}$ ) of an isotope  $j$  will be

$$Y_j = C \sum_i \frac{f_i}{A_{ti}} \int \frac{d\phi}{dE} \sigma_{ij}(E) dE, \quad (2)$$

where  $C$  is a normalisation factor and  $\sigma_{ij}(E)$  is the cross-section (mb) for the target-product isotope pair at energy  $E$  (MeV). The integral is over the required energy range of the input beam spectrum, while the sum is over all of the target isotopes. Here,

$$C = N_A \times 24 \times 3600 \times 10^{-24}, \quad (3)$$

where  $N_A$  is Avogadro's number ( $6.022 \times 10^{23} \text{mol}^{-1}$ ), the next two numbers convert the production rate from per second to per day, while the last factor accounts for the different units of area used for the flux ( $\text{cm}^2$ ) and cross-section (mb) quantities, as well as the unit of mass used for the atomic number  $A_{ti}$  (converting g to kg). If the target is exposed to the (continuous) beam for a time  $t_{\text{exp}}$  (days), then the yield rate ( $\text{kg}^{-1} \text{day}^{-1}$ ) of the radioactive product isotope  $j$  with a half-life of  $t_{1/2}$  (days) is given by

$$Y_j^{\text{exp}} = Y_j (1 - e^{-\lambda_j t_{\text{exp}}}), \quad (4)$$

where  $\lambda_j = \ln 2/t_{1/2}$  and assuming no chained decays. If the target is removed from the beam and the product isotope is allowed to decay for a time  $t_{\text{dec}}$  (days), then the final product yield rate is

$$Y_j^{\text{dec}} = Y_j^{\text{exp}} e^{-\lambda_j t_{\text{dec}}} = Y_j (1 - e^{-\lambda_j t_{\text{exp}}}) e^{-\lambda_j t_{\text{dec}}}. \quad (5)$$

Here, we only consider product isotopes with half-lives greater than one day. However, there are many short-lived isotopes which can decay to these, and they are included in the cross-section and yield calculations as ‘‘side-branch nuclei’’. For example, consider the decay chain to the long-lived isotope  $^{14}\text{C}$  ( $t_{1/2} = 5730$  years):  $^{14}\text{Be} \rightarrow ^{14}\text{B} + e^- + \bar{\nu}_e$  ( $t_{1/2} = 4$  ms) and  $^{14}\text{B} \rightarrow ^{14}\text{C} + e^- + \bar{\nu}_e$  ( $t_{1/2} = 14$  ms). This means that both  $^{14}\text{Be}$  and  $^{14}\text{B}$  are considered side-branches of  $^{14}\text{C}$ , and their cross-sections and yields will contribute to those for  $^{14}\text{C}$ .

#### 5. Code structure

The code, written in C++ to take advantage of object-oriented design principles, is split into two main sections; the first part performs the calculation of the cross-sections (Eq. 1) and production rates (Eq. 2), while the second part calculates the final yields of the radioactive isotope products (Eq. 5). The basic structure of the code, designed to work in the Unix environment, is described below. Details on how to build and run the code are found in the README file of the computer package [8].

##### 5.1. Input

There are several inputs that are necessary for the cross-section and yield calculations. They are the target isotopes, a list of all allowed product isotopes, the input beam spectrum, as well as the beam exposure and target cooling times. These are specified by the ActAbsInput abstract interface, which is a base class that contains several pure virtual functions that must be implemented by any derived classes, such as ActInput. Figure 3 shows a simplified version of the overall program flow.

The class ActTarget defines the target element, together with its isotopes and their relative abundance fractions  $f_i$  (such that  $\sum_i f_i = 1$ ). If a target is comprised of many elements (each with their own isotopes), then the code must be run as many times as is necessary to get the results for each target element. The results must then be combined at the end by the user.

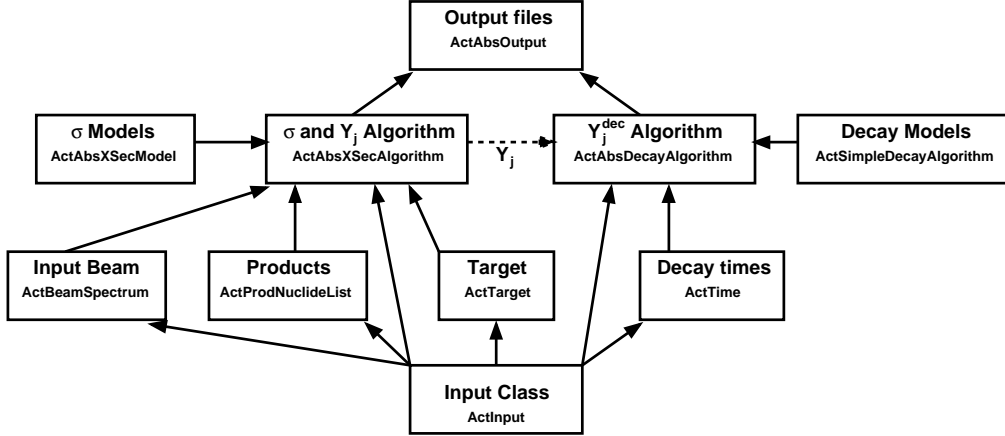


Fig. 3. Diagram showing a simplified version of the program flow and C++ class structure. The input specifies the beam spectrum, the list of product and target isotopes, the decay times, as well as algorithms for the cross-section and yield calculations. These algorithms use the various inputs with the required cross-section and decay yield models to generate the output files for further analysis.

The list of allowed products is defined in the `ActProdNuclideList` class, which is built from an ASCII text file (“decayData.dat”) containing a complete list of radioactive isotopes found in the periodic table with half-lives equal to or greater than one day. All target and product isotopes are represented by `ActNuclide` objects, which store the atomic ( $Z$ ) and mass ( $A$ ) numbers as well as the half-life  $t_{1/2}$ . Product nuclide objects also contain the  $Z$  and  $A$  values of any side-branch nuclei (defined at the end of Section 4). Each nuclide is created only once by the factory class `ActNuclideFactory`, independent of how many times it is used in the code.

The input beam spectrum is defined through the abstract class `ActBeamSpectrum`, in which the flux ( $d\phi/dE$  in units of  $\text{cm}^{-2}\text{s}^{-1}\text{MeV}^{-1}$ ) must be implemented by any derived class. At present, the only available input beam is the cosmic ray spectrum shown in Fig. 2, which is assumed to be valid for neutrons and protons. The `ActBeamSpectrum` class also stores the energy range and bin width  $\Delta E$ , which are used to calculate the integral in Eq. 2, as well as the atomic number  $Z_{\text{beam}}$  and mass number  $A_{\text{beam}}$  of the beam particles, both equal to unity for cosmic ray protons.

The final required input variables are the time  $t_{\text{exp}}$  that the target is exposed to the beam and the time elapsed after the target is removed from the beam (decay or cooling time  $t_{\text{dec}}$ ), both in units of days. These are stored within the simple `ActTime` class.

The set-up of the calculations is managed by the `ActInput` class, as mentioned earlier, which prompts

the user to provide the required inputs using the standard C++ input streamer “cin”. Examples are provided in the README file of the package [8].

The algorithms for calculating the cross-sections and yields must also be selected in the input class. At present, the cross-sections are calculated using Eq. 1 (with any available data tables as described in Section 3) by the `ActSTXSecAlgorithm` class, while the yields are evaluated using Eq. 5 by the `ActSimpleDecayAlgorithm` class. We now describe how these algorithms work.

## 5.2. Cross-sections

The calculation of the cross-sections between all target and product isotope pairs is controlled by the `ActIsotopeProduction` class, which retrieves information about the target, the list of product isotopes, and the beam energy spectrum from the input class.

The cross-sections for each target isotope ( $Z_t, A_t$ ) are calculated using the `ActProdXSecData` utility class. This loops over all available product isotopes ( $Z, A$ ) and calculates the cross-section for each energy bin in the input beam spectrum. The values of  $Z$  and  $A$  must satisfy the requirements  $Z \leq Z_t + Z_{\text{beam}}$  and  $A \leq A_t + A_{\text{beam}} - 1$ , which ensure that there are at least two isotope products in each reaction, i.e. the cross-sections for any  ${}^A_Z X + p \rightarrow {}^{A+1}_{Z+1} Y + \gamma$  reactions are not calculated. Any side-branch nuclei are included in the cross-section calculations. The energy of the reaction must be larger than a

threshold energy, typically of order 10 MeV, defined as the mass excess from the target-product reaction, and is calculated using the semi-empirical formula from Seeger [9]. Otherwise, the cross-section is set to zero and the next energy bin is considered. This requirement avoids calculating the cross-section of resonances for low-energy ( $E \lesssim 10$  MeV) reactions, which is beyond the scope of this work.

The required cross-section is retrieved from the `ActSTXSecAlgorithm` class. This first checks if there are any cross-section data for the target-product isotope pair at the given energy (above threshold). If no such data exists, or the cross-section is too small ( $< 0.001$  mb, for example), then Eq. 1 is used to calculate the cross-section. The algorithm selects which calculation region in Fig. 1 is appropriate, i.e. what parameters are needed for Eq. 1, and calls the class that implements the specific Silberberg-Tsao model, such as spallation, fission or peripheral reactions. The total cross-section is then just the sum of  $\sigma(E)$  over all energy bins. The calculations do not distinguish between ground or metastable states for the product nuclei.

### 5.3. Yields

The production rates of the isotopes (Eq. 2) are calculated by `ActIsotopeProduction` when the cross-sections are evaluated. Following Eq. 2, the production rate at the energy  $E_k$  is given by

$$y_j(E_k) = C \sum_i \frac{f_i}{A_{ti}} \frac{d\phi}{dE} \sigma_{ij}(E_k) \Delta E, \quad (6)$$

where  $\Delta E$  is the energy bin width from the input beam spectrum. The total production rate is given by the sum of  $y_j(E_k)$  over all energy bins

$$Y_j = C \sum_i \frac{f_i}{A_{ti}} \left[ \sum_k \frac{d\phi}{dE} \sigma_{ij}(E_k) \Delta E \right], \quad (7)$$

where the sum over  $k$  specifies the required energy bin range. The `ActSimpleDecayAlgorithm` class implements Eq. 5 to find the final yield  $Y_j^{\text{dec}}$  for each product isotope  $j$  from the given exposure and decay times. This simple calculation ignores any chained decays, in which isotopes can decay to several other long-lived nuclei, or when isotopes can be made from multiple decays. However, short-lived isotopes are included in the final product yields through the use of the side-branch nuclei, as mentioned in Section 4.

### 5.4. Output

The results of the cross-section and yield calculations are stored in output files using the abstract interface `ActAbsOutput`, which contains several pure virtual functions that must be implemented by any derived class, such as `ActStreamOutput` for ASCII text output or `ActROOTOutput` for ROOT [10] output. These classes must be able to deal with three different formats: lines of text (character strings or `ActString` objects), tables of numbers (`ActOutputTable` objects) and graphs (`ActAbsGraph` objects). The cross-section and yield algorithms are not concerned with specific formats of output files; they only create tables and graphs which are then passed onto the output class, which decides how to write out the information in whatever format is required for further analysis.

The `ActOutputTables` store rows of numbers, where each column represents a specific variable with its own unique label. Graphs are made up of a series of points, which are represented by `ActGraphPoint` objects that can store several  $y$  values for a given  $x$  co-ordinate, each with their own labels and units. For example, `ActXSecGraph` has  $x$  equal to the energy  $E$  (MeV),  $y_1$  equal to the cross-section value (mb) and  $y_2$  equal to the production rate  $Y_j$  ( $\text{kg}^{-1} \text{day}^{-1}$ ). `ActDecayGraphs` contain points storing the elapsed time (in days) and the corresponding isotope yield:  $(x, y) = (t_{\text{exp}}, Y_j^{\text{exp}})$  or  $(t_{\text{exp}} + t_{\text{dec}}, Y_j^{\text{dec}})$ .

Each output class must be able to deal with two output files; the first one contains details from the cross-section and production rate calculations, while the second one contains the yields from the isotope decay algorithm.

The total cross-section (mb) and production rate ( $\text{kg}^{-1} \text{day}^{-1}$ ) are stored in the cross-section output file. Also stored is the cross-section and production rate as a function of input beam energy (MeV), but only if a flag controlling the level of output detail is set appropriately. Again, the output class must determine what to do when the level of detail is changed; the cross-section and yield calculations are not affected by this. Finally, a summary table of the yields of each product isotope at the start and end of the decay period ( $t_{\text{exp}}$  and  $t_{\text{exp}} + t_{\text{dec}}$ ), weighted over all target isotopes, is written to the decay output file.

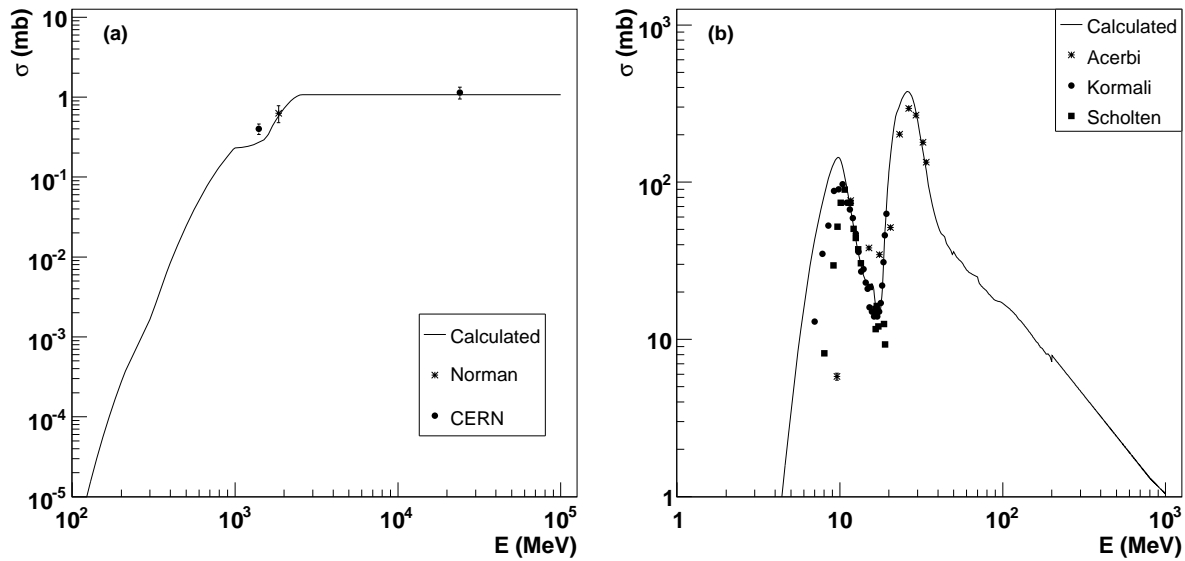


Fig. 4. Cross-section as a function of energy for (a)  $^{60}\text{Co}$  and (b)  $^{128}\text{I}$  produced by protons in natural tellurium. Data sets in (a) are from Norman [12] and CERN [13]. Data points in (b) are from Acerbi [14], Kormali [15] and Scholten [16].

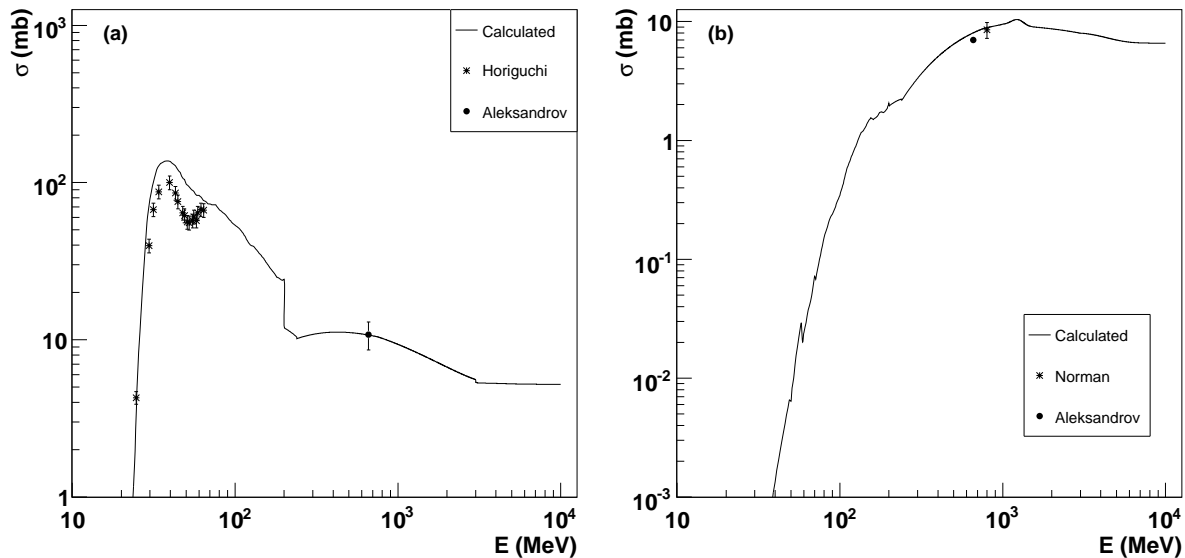


Fig. 5. Cross-section as a function of energy for (a)  $^{68}\text{Ge}$  and (b)  $^{60}\text{Co}$  produced by protons in natural germanium. Data points are from Norman [12], Horiguchi [17] and Aleksandrov [18].

## 6. Comparisons between measurements and calculations

The calculations of the cross-sections have been benchmarked using experimental data from the EXFOR database [4] for natural tellurium, germanium and copper targets. The results of the calculations agree in general with those shown in various reports from the IDEA collaboration [11]. Figures 4 to 6

show the calculated cross-section graphs of several isotopes along with the data points from experimental results [4]. The agreement between calculations and experimental results is not uniform; some results agree very well (<50% relative difference), others agree within a factor of two, but there are also discrepancies up to a factor of 10 or more. It is clear that some of the MENDL-2P [5] cross-sections for energies between  $\sim 10$  MeV to 200 MeV do not agree

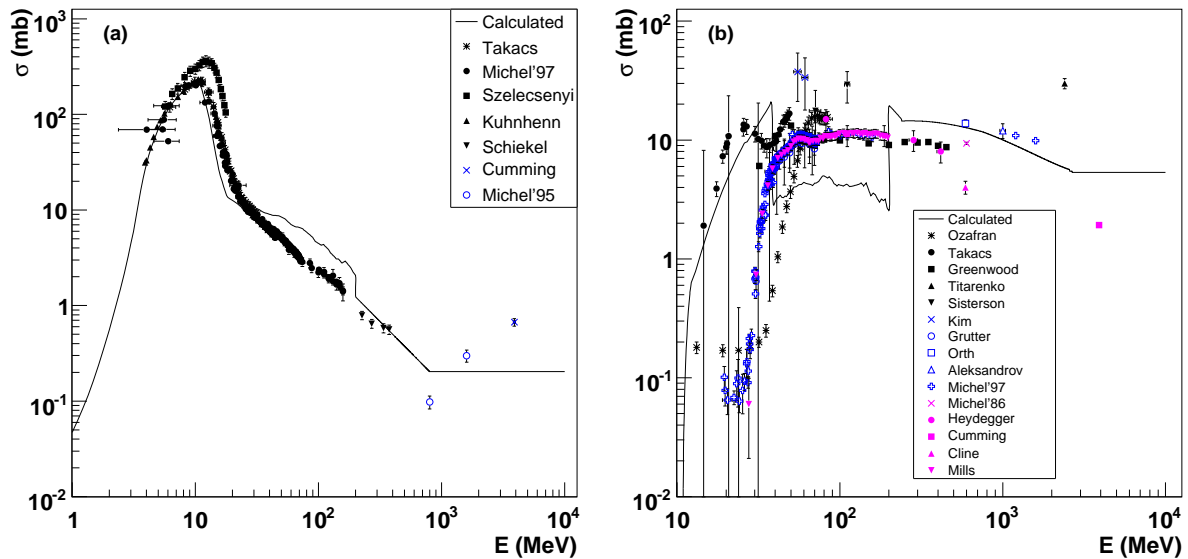


Fig. 6. Cross-section as a function of energy for (a)  $^{65}\text{Zn}$  and (b)  $^{60}\text{Co}$  produced by protons hitting a natural copper target. The calculation of the  $^{60}\text{Co}$  cross-section for energies in the range 40–200 MeV uses the MENDL-2P data tables, which underestimate the values obtained by various experiments. Data points shown in (a) are from Takács [19], Michel'97 [20], Szelecsényi [21], Kuhnhenh [22], Schiekel [23], Cumming [24] and Michel'95 [25]. Data points shown in (b) are from Ozafran [26], Takács [27], Greenwood [28], Titarenko [29], Sisterson [30], Kim [31], Grütter [32], Orth [33], Aleksandrov [34], Michel'86 [35], Heydegger [36], Cline [37] and Mills [38].

very well with experimental results, such as those shown in Fig. 6. Obviously, the agreement will improve if the MENDL-2P data tables are updated accordingly. In fact, the user is free to use other experimental data for the cross-section tables instead of those from the MENDL-2P database. Instructions on creating self-made data tables are provided in the README file of the package [8].

Table 1

Induced activities  $Y_j^{\text{dec}}$  ( $\mu\text{Bq kg}^{-1}$ ) of  $\text{TeO}_2$  for three nuclides assuming four months of exposure to cosmic rays and two years of decay in a shielded underground environment. There are two calculations from the IDEA Collaboration [11]; IDEA<sup>a</sup> uses the cosmic-ray flux distribution  $\phi$  from Fig. 2 while IDEA<sup>b</sup> uses the distribution from Ziegler [39].

	$^{60}\text{Co}$	$^{125}\text{Sb}$	$^{124}\text{Sb}$
CUORE [40]	0.20	15	0.05
IDEA <sup>a</sup> [11]	0.02	$6 \pm 6$	$0.01 \pm 0.03$
IDEA <sup>b</sup> [11]	0.02	$22 \pm 15$	$0.05 \pm 0.06$
ACTIVIA	0.03	6	0.02

Comparisons have been made between the induced activity calculated by ACTIVIA with results shown in reports from the IDEA collaboration [11] for several targets and isotope products. Table 1 shows an example of the calculated induced activities for  $\text{TeO}_2$  exposed to cosmic rays at sea level for

four months and shielded underground for a further two years. Note that the ACTIVIA result for  $^{60}\text{Co}$ , which predicts a production rate  $Y_j = 0.8 \mu\text{Bq kg}^{-1}$  (YIELDX [41] predicts  $0.7 \mu\text{Bq kg}^{-1}$ ), is a factor of 10 lower than the estimate obtained by the CUORE collaboration [40] (using a modified version of COSMO [42]) owing to the improved calculation of the cross-section (see Fig. 4). Tables 2 and 3 show the induced rates of isotope production by cosmic rays at sea level for natural and enriched germanium, respectively. One can see that there are differences between the various estimates presented in the tables. For example, the ACTIVIA results using the MENDL-2P data tables shown in Table 2 are generally quite close to those from Avignone [43], but are approximately a factor of two less than those from HMS-ALICE [44] and YIELDX [41] estimates and those from Klapdor-Kleingrothaus [45]. Similar discrepancies between measurements and calculations are also found for the enriched germanium yield estimates shown in Table 3. Table 4 shows the isotope production yields for natural copper. Two of the ACTIVIA results agree with those from Baudis and Schnee [49], but all of the calculated yields are less than those estimated by the IDEA group, whose calculations included the MENDL low energy ( $E \lesssim 10 \text{ MeV}$ ) neutron data [50]. Most of the cobalt results from Formaggio [48] in Tables 2

Table 2

Induced rates of isotope production  $Y_j$  ( $\text{kg}^{-1} \text{day}^{-1}$ ) in natural germanium at sea level. The values from Avignone [43] are separated into Monte Carlo simulation (MC) and experimental (exp) results.

	$^{68}\text{Ge}$	$^{60}\text{Co}$	$^{65}\text{Zn}$	$^{58}\text{Co}$	$^{57}\text{Co}$	$^{56}\text{Co}$	$^{54}\text{Mn}$	$^{63}\text{Ni}$	$^{55}\text{Fe}$
HMS-ALICE, YIELDX [44,41]	89.0	4.8	77.0	14.0	9.7	3.0	7.2	5.2	8.0
Avignone [43] (MC)	29.6	—	34.4	5.3	4.4	—	2.7	—	—
Avignone [43] (exp)	$30.0 \pm 7.0$	—	$38.0 \pm 6.0$	$3.5 \pm 0.9$	$2.9 \pm 0.4$	—	$3.3 \pm 0.8$	—	—
Klapdor-Kleingrothaus [45]	58.4	6.6	79.0	16.1	10.2	—	9.1	4.6	8.4
Miley [46]	26.5	4.8	30.0	4.4	0.5	—	—	—	—
Barabanov [47]	81.6	2.9	—	—	—	—	—	—	—
Formaggio [48]	29.5	—	—	154.0	—	5.4	4.8	—	—
ACTIVIA	45.8	2.8	29.0	8.5	6.7	2.0	2.7	1.6	3.4

Table 3

Induced rates of isotope production  $Y_j$  ( $\text{kg}^{-1} \text{day}^{-1}$ ) in enriched germanium (86%  $^{76}\text{Ge}$  and 14%  $^{74}\text{Ge}$ ) at sea level.

	$^{68}\text{Ge}$	$^{60}\text{Co}$	$^{65}\text{Zn}$	$^{58}\text{Co}$	$^{57}\text{Co}$	$^{54}\text{Mn}$	$^{63}\text{Ni}$	$^{55}\text{Fe}$
HMS-ALICE, YIELDX [44,41]	13.0	6.7	24.0	6.2	2.3	5.4	6.0	2.3
Avignone [43]	0.9	—	6.4	1.8	1.0	1.4	—	—
Miley [46]	1.2	3.5	6.0	1.6	0.1	—	—	—
Barabanov [47]	5.8	3.3	—	—	—	—	—	—
ACTIVIA	7.6	2.4	10.4	5.5	2.9	2.2	1.4	1.6

Table 4

Induced rates of isotope production  $Y_j$  ( $\text{kg}^{-1} \text{day}^{-1}$ ) in natural copper at sea level. For the ACTIVIA calculations, there are two sets of values; those from only the semi-empirical formulae and those that also include the MENDL-2P data.

	$^{56}\text{Co}$	$^{57}\text{Co}$	$^{58}\text{Co}$	$^{60}\text{Co}$	$^{54}\text{Mn}$	$^{59}\text{Fe}$	$^{46}\text{Sc}$
IDEA [11]	22.9	88.3	159.6	97.4	32.5	6.5	3.8
Baudis [49]	—	30.5	—	25.7	134.2	—	—
Formaggio [48]	972.3	—	131.5	2675.5	52.2	—	—
ACTIVIA formulae only	8.7	32.5	56.6	26.3	14.3	4.2	3.1
ACTIVIA with MENDL-2P	14.1	36.4	38.1	9.7	12.5	1.8	3.1

and 4 are systematically higher than those from other analyses; it is unclear why this is the case.

One important source of uncertainty in the production rates is the cosmic ray spectrum, where discrepancies around a factor of two can be explained by differences between the parameterisations used in various calculations (such as the spectrum shown in Fig. 2 used in ACTIVIA) and cosmic ray fluxes (which depend on geographic location and time) measured by various experiments.

Another important issue is that the semi-empirical formulae must be able to predict the cross-sections of isotope production over a wide range of isotope masses and input beam energies. As shown in Fig. 1, there are several physical processes that can take place in nuclear reactions. Each process must be described by a set of formulae that can adequately predict the cross-section for any

given isotope and beam energy. Obviously, this can only be accomplished if there is enough experimental data to derive such functions and obtain all relevant parameters with sufficient accuracy. The data used by Silberberg and Tsao did not cover all possible isotopes and energies, which limits the predictive power of the formulae for various cases. As can be seen in Figs. 4 and 5, some isotopes have very few measurements available. More experimental data are needed so that improvements can be made to semi-empirical formulae, data tables and Monte Carlo simulations for isotope production calculations.

## 7. Code modifications and extensions

The code is structured so that modifications or extensions can be made to several components of the



cross-section and yield calculations whilst keeping the overall framework intact.

Different input beam spectra can be used by including classes that inherit from `ActBeamSpectrum`; the appropriate spectrum must be chosen by the input class. For example, a class describing the flux of an ion beam can be provided, although the formulae for calculating the cross-sections of products from such a beam would need to be implemented as well. The beam spectrum class also needs to specify the energy range and bin width that are used to calculate the integral in Eq. 2, as well as the atomic number  $Z_{\text{beam}}$  and mass number  $A_{\text{beam}}$  of the beam particles.

The “decayData.dat” file contains a list of all available isotope products with half-lives greater than one day, as well as their side-branch nuclei. Other isotopes, with shorter half-lives, can be added to this data file. The code will calculate the cross-sections and yields for these nuclei automatically without any changes necessary to the source code. However, any side-branches matching the new isotopes would need to be removed to avoid double counting.

At present, the cross-sections are calculated by the `ActSTXSecAlgorithm` class using a combination of values from (MENDL) data tables as well as semi-empirical formulae from Silberberg and Tsao. Cross-section models for processes like spallation and fission are implemented in their own classes, making it easier to update their parameters or formulae when necessary. New nuclear models can be added to the `ActSTXSecAlgorithm` class if required.

Other cross-section algorithms can be specified, as long as they inherit from the base class `ActAbsXSecAlgorithm` and are selected appropriately in the input class. For example, new algorithms may be needed to specify cross-section formulae when beams other than cosmic rays (protons/neutrons) are used.

Other decay algorithms could be written, such as those that take into account chained decays, if they follow the `ActAbsDecayAlgorithm` abstract interface, which has access to the list of possible isotope products (`ActProdNuclideList`), as well as the definition of the target (`ActTarget`) and the `ActProdXSecData` results it stores (the target-product cross-sections). `ActNuclide` objects can be retrieved from the target and product list to take care of any bookkeeping required for chained decay algorithms. Note that the decay algorithm is separated from the cross-section calculations, allowing the possibility of using different decay algorithms for the same initial production yields, provided they are selected appro-

priately by the input class.

Changes can be made to how the calculations are set up. The default `ActInput` class uses standard C++ input/output commands to get the necessary information from the user. Other classes using different input formats, such as XML files, could be implemented. However, they must all derive from the abstract `ActAbsInput` interface, and provide all required inputs (beam spectrum, target and product isotopes, decay times and selection of cross-section and decay yield algorithms).

At present there are two output formats available: ASCII text files and ROOT [10] files. Other output formats could be written, provided the classes follow the abstract `ActAbsOutput` interface and know how to deal with lines of text, tables of data (`ActOutputTables`) and graphs (`ActAbsGraph` objects).

## 8. Summary

We have presented the ACTIVIA C++ computer package that can be used to calculate target-product cross-sections and the production and decay yields of isotopes from cosmic ray activation. Cross-sections are calculated using a combination of semi-empirical formulae, assumed to be the same for proton and neutron beams, and ASCII tables of (experimental) data.

The basic structure of the code, designed to work in the Unix environment, has been presented. It is structured so that modifications or extensions can be made to several components of the cross-section and yield calculations whilst keeping the overall framework intact. Since ACTIVIA uses only formulae or data tables to calculate cross-sections, and does not simulate individual particles and their interactions, it is easier to use than full Monte Carlo simulation computer packages such as GEANT4 [51], while it is more extensible than similar FORTRAN-based codes like COSMO [42]. At present, the code is limited to only calculating the isotope production cross-sections and yields for one given target element (with its various isotopes); for targets made up of several elements, the code must be run separately for each and the results combined at the end by the user. Results from the calculations can be written out as ASCII text or stored within ROOT [10] files.

We have compared isotope production results from ACTIVIA against experimental data and estimates from other calculations; in general, they agree within a factor of two. It is possible to change or extend the algorithms and formulae used to cal-

culate the cross-sections and isotope yields. Finally, we have discussed ways of modifying the code such that it may be used in applications other than calculating yields of cosmogenic isotope products.

#### Acknowledgments

We thank Tom Latham and Ben Morgan for useful discussions about the code design. We also thank the OECD Nuclear Energy Agency, France, for providing us with the MENDL-2P data tables. This work is supported by the Science and Technology Facilities Council (United Kingdom).

#### References

- [1] R. Silberberg, C.H. Tsao, *Astrophys. J. Suppl.* 220 (I) 25 (1973) 315; R. Silberberg, C.H. Tsao, *Astrophys. J. Suppl.* 220 (II) 25 (1973) 335.
- [2] R. Silberberg, C.H. Tsao, *Astrophys. J. Suppl.* 35 (1977) 129; R. Silberberg, C.H. Tsao, J.R. Letaw, *Astrophys. J. Suppl.* 58 (1985) 873; R. Silberberg, C.H. Tsao, J.R. Letaw, in: *Proceedings of the 20th International Cosmic Ray Conference, Moscow, vol. 2, 1987, p. 133*; R. Silberberg, C.H. Tsao, *Phys. Rep.* 191 (1990) 351; R. Silberberg, C.H. Tsao, A.F. Barghouty, *Astrophys. J.* 501 (1998) 911.
- [3] A.Yu. Konobeyev, Yu.A. Korovin, *Nucl. Instr. and Meth. B* 82 (1993) 103.
- [4] The Experimental Nuclear Reaction Data (EXFOR) database at <http://www-nds.iaea.org/exfor/>
- [5] Yu.N. Shubin, et al., MENDL-2P: Proton Reaction Data Library for Nuclear Activation (Medium Energy Nuclear Data Library) IAEA-NDS-204, 1998.
- [6] T.W. Armstrong, K.C. Chandler, J. Barish, *J. Geophys. Res.* 78 (1973) 2715.
- [7] N. Gehrels, *Nucl. Instr. and Meth. A* 239 (1985) 324.
- [8] The ACTIVIA package is available for download at <http://www.warwick.ac.uk/go/activia>
- [9] P.A. Seeger, *Nucl. Phys.* 25 (1961) 1.
- [10] R. Brun, F. Rademakers, *Nucl. Instr. and Meth. A* 389 (1997) 81. See also <http://root.cern.ch>
- [11] Integrated double-beta decay European activities at <http://idea.dipscfm.uninsubria.it>
- [12] E.B. Norman, et al., *Nucl. Phys. B Proc. Suppl.* 143 (2005) 508.
- [13] Unpublished preliminary results from irradiation experiments at CERN.
- [14] E. Acerbi, et al., *Int. J. Appl. Radiat. Isot.* 26 (1975) 741.
- [15] S.M. Kormali, D.L. Swindle, E.A. Schweikert, *J. Radioanal. Nucl. Chem.* 31 (1976) 437.
- [16] B. Scholten, S.M. Qaim, G. Stöcklin, *Int. J. Appl. Radiat. Isot.* 40 (1989) 127.
- [17] T. Horiguchi, et al., *Int. J. Appl. Radiat. Isot.* 34 (1983) 1531.
- [18] Yu.V. Aleksandrov, et al., *Bull. Russ. Acad. Sci. Phys.* 59 (1995) 895.
- [19] S. Takács, et al., *Nucl. Instr. and Meth. B* 188 (2002) 106.
- [20] R. Michel, et al., *Nucl. Instr. and Meth. B* 129 (1997) 153.
- [21] F. Szelecsényi, et al., *Nucl. Instr. and Meth. B* 174 (2001) 47.
- [22] J. Kuhnhenh, Ph.D. Thesis, University of Köln, Germany, 2001.
- [23] Th. Schiekkel, et al., *Nucl. Instr. and Meth. B* 114 (1996) 91.
- [24] J. B. Cumming, et al., *Phys. Rev. C* 10 (1974) 739.
- [25] R. Michel, et al., *Nucl. Instr. and Meth. B* 103 (1995) 183.
- [26] M.J. Ozafran, et al., *J. Radioanal. Nucl. Chem.* 131 (1989) 467.
- [27] S. Takács, et al., *Nucl. Instr. and Meth. B* 251 (2006) 56.
- [28] L.R. Greenwood, R.K. Smither, *Prog. Rep. U.S. Department of Energy, Fusion Energy Series, No. 0046, 18 (1984) 11.*
- [29] Yu.E. Titarenko, et al., *Proc. AccApp'03, San Diego, California, nucl-ex/0305026 (2003).*
- [30] J.M. Sisterson, et al., *Nucl. Instr. and Meth. B* 240 (2005) 617.
- [31] E.J. Kim, et al., *J. Nucl. Sci. Tech.* 36 (1999) 29.
- [32] A. Grütter, *Nucl. Phys. A* 383 (1982) 98.
- [33] C.J. Orth, et al., *J. Inorg. Nucl. Chem.* 38 (1976) 13.
- [34] Yu.V. Aleksandrov, et al., *Bull. Russ. Acad. Sci. Phys.* 54 (1990) 161.
- [35] R. Michel, et al., *Nucl. Instr. and Meth. B* 16 (1986) 61.
- [36] H.R. Heydegger, C.K. Garrett, A. Van Ginneken, *Phys. Rev. C* 6 (1972) 1235.
- [37] J.E. Cline, E.B. Nieschmidt, *Nucl. Phys. A* 169 (1971) 437.
- [38] S.J. Mills, G.F. Steyn, F.M. Nortier, *Int. J. Appl. Radiat. Isot.* 43 (1992) 1019.
- [39] J.F. Ziegler, *IBM J. Res. Dev.* 42 (1998) 117.
- [40] R. Ardito, et al., *hep-ex/0501010 (2005).*
- [41] Code written by Silberberg and Tsao implementing their own semi-empirical formulae described in Refs. [1,2].
- [42] C.J. Martoff, P.D. Lewin, *Comput. Phys. Commun.* 72 (1992) 96. Code modified by Y.A. Ramachers.
- [43] F.T. Avignone, et al., *Nucl. Phys. B Proc. Suppl.* 28 (1) (1992) 280.
- [44] M. Blann, *Phys. Rev. C* 54 (1996) 1341; M. Blann, M.B. Chadwick, *Phys. Rev. C* 57 (1998) 233.
- [45] H.V. Klapdor-Kleingrothaus, et al., *Nucl. Instr. and Meth. A* 481 (2002) 149.
- [46] H.S. Miley, et al., *Nucl. Phys. B Proc. Suppl.* 28 (1) (1992) 212.
- [47] I. Barabanov, et al., *Nucl. Instr. and Meth. B* 251 (2006) 115.
- [48] J.A. Formaggio, C.J. Martoff, *Ann. Rev. Nucl. Part. Sci.* 54 (2004) 361.
- [49] L. Baudis, R.W. Schnee, *Dark Matter Experiments NUSL White Paper, 2002.*
- [50] Yu.N. Shubin, et al., MENDL-2: Neutron Reaction Data Library for Nuclear Activation (Medium Energy Nuclear Data Library) IAEA-NDS-136, 1995.
- [51] S. Agostinelli, et al., *Nucl. Instr. and Meth. A* 506 (2003) 250.